Journal of Orthopaedic Translation 36 (2022) 120–131

Contents lists available at ScienceDirect

Journal of Orthopaedic Translation

journal homepage: www.journals.elsevier.com/journal-of-orthopaedic-translation

An injectable pH neutral bioactive glass-based bone cement with suitable bone regeneration ability

Xibing Zhang [a,1], Yanlin Chen [b,1], Jiaming Fu [a,1], Qiuhong Chen [a], Yang Li [c], Canliang Fang [c], Chenglong Li [b], Liang Wang [a], Dong Qiu [d,e,**], Zhongmin Zhang [a,b,*]

[a] Department of Orthopedics, The Third Affiliated Hospital, Southern Medical University, Academy of Orthopedics, Guangzhou, 510630, PR China
[b] Division of Spine Surgery, Department of Orthopedics, Nanfang Hospital, Southern Medical University, Guangzhou, 510080, PR China
[c] Songshan Lake Materials Laboratory, Dongguan, Guangdong, 523808, PR China
[d] Beijing National Laboratory for Molecular Sciences, CAS Research/Education Center for Excellence in Molecular Sciences, Institute of Chemistry, Chinese Academy of Sciences, Beijing, 100190, PR China
[e] University of Chinese Academy of Sciences, Beijing, 100190, PR China

ARTICLE INFO

Keywords:
Bone regeneration
Bioactive glass
Injectable bone cement
Neutral pH

ABSTRACT

Background: As a class of promising bone augmentation materials, bone cements have attracted particular attention. Due to various limitations, the current bone cements are still imperfect. In this study, an injectable pH neutral bioactive bone cement (PSC/CSC) was developed by mixing phosphosilicate bioactive glass (PSC) and α-calcium sulfate hemihydrate (CSH), with the goal of optimizing bone defects repairs.
Methods: A range of compositions (PSC/CSC: 10P/90C, 30P/70C, 50P/50C) were developed and their physicochemical properties evaluated. Their bone regeneration ability was compared to those of two widely used bone cements as controls (calcium phosphate cement (CPC) and Genex®) in rabbit femoral condyle bone defect models for 4, 8 and 12 weeks. Based on physicochemical properties and *in vivo* bone regeneration ability, the PSC/CSC exhibited the best outcomes was selected. Then, *in vitro*, the effects of selected PSC/CSC, CPC and Genex® extracts on MC3T3-E1 cell proliferation, migration and osteogenesis as well as angiogenesis of HUVECs were examined.
Results: Based on physicochemical properties, the 30P/70C formula exhibited suitable operability and compressive strength (3.5 ± 0.3 MPa), which fulfilled the requirements for cancellous bone substitutes. *In vivo*, findings from micro-CT and histological analyses showed that the 30P/70C formula better promoted bone regeneration, compared to 10P/90C, 50P/50C, CPC and Genex®. Hence, 30P/70C was selected as the ideal PSC-based cement. *In vitro*, the 30P/70C extracts showed better promotion of cell viability, alkaline phosphatase (ALP) activity, calcium mineral deposition, mRNA and protein expression levels of osteogenesis in MC3T3-E1 cells, further supporting its superiority. Meanwhile, the 30P/70C extracts also showed better stimulation of HUVECs proliferation and angiogenesis.
Conclusion: The new composite cement, 30P/70C, is a favorable bioactive glass-based bone cement with suitable operability, compressive strength and bone regeneration ability.
The translational potential of this article: Clinically, treatment of large bone defects is still a major challenge for orthopaedic trauma. We showed that 30P/70C has the potential to be clinically used as an injectable cement for rapid bone repairs and reconstruction of critical sized bone defects.

1. Introduction

Due to their convenient handling properties, bone cements have been successfully used as injectable bone substitutes [1]. They can be used for bonding, filling and repairing free-shape bone defects [2]. Calcium sulfate cement (CSC) with low temperature self-setting ability has enjoyed a long history of clinical applications as injectable bone augmentation [3]. It is associated with good biocompatibility, osteoconductivity and

* Corresponding author. Department of Orthopedics, The Third Affiliated Hospital, Southern Medical University, Academy of Orthopedics, Guangzhou, 510630, PR China.
** Corresponding author. University of Chinese Academy of Sciences, Beijing, 100190, PR China.
E-mail addresses: dqiu@iccas.ac.cn (D. Qiu), nfzzm@163.com (Z. Zhang).
[1] These authors contributed equally to this work.

https://doi.org/10.1016/j.jot.2022.05.011
Received 8 February 2022; Received in revised form 21 May 2022; Accepted 27 May 2022

moderate X-ray radiopacity properties [4]. In addition, it can be used as a vehicle to deliver drugs, growth factors or as an additive to modulate the degradation rate when blended with other biomaterials [3]. However, CSC has a rapid degradation rate. The degradation rate of CSC is faster than new bone regeneration rate, thus, it may not provide adequate mechanical support [5,6]. In addition, in the early stages, CSC cannot form a chemical bond with host bone tissues because it has poor bioactivity [7]. Therefore, strategies to slow down the degradation rate and improve the bioactivity of CSC should be developed and implemented.

Bioactive glass (BG) is a promising artificial biomaterial for bone repairs. It has excellent biocompatibility, bioactivity and osteoinductivity properties [8]. Moreover, its degradation rate is much slower than that of calcium sulfate. Therefore, BG blended with calcium sulfate showed better osteoinductivity and stimulation of bone ingrowth [5,9]. However, the improvements were limited, because the basic nature of conventional BG (pH higher than 9) interfered with hydration reactions and the setting behavior of calcium sulfate [7].

Recently, a pH neutral phosphosilicate (PSC) BG was developed, which can maintain a stable pH of around 7.4 when reacting with physiological solutions [10]. Osteogenesis of PSC is superior and its degradation rate low [7,11]. Therefore, we wish to develop a PSC-based bone cement (PSC/CSC) by mixing PSC and α-calcium sulfate hemihydrate (CSH), based on the hypothesis that, with a proper formula, PSC/CSC can optimize bone defects repair.

In the present study, we formulated a series of PSC/CSCs and evaluated their physicochemical properties. Their *in vivo* bone defects repair performances were compared to those of two widely used bone cements, calcium phosphate cement (CPC) and Genex®. Based on the above results, the best proportion of PSC/CSCs was selected. Then, *in vitro*, effects of the selected PSC/CSC, CPC and Genex® extracts on osteogenesis of MC3T3-E1 cells and angiogenesis of HUVECs were assessed.

2. Materials and methods

2.1. Materials

PSC was kindly donated by Wooquick company (Taizhou, China) [10] and ground into particles with a diameter of less than 38 μm. CSH was purchased from Sigma–Aldrich (St. Louis, MO, USA). CPC, which was composed of β-tricalcium phosphate, calcium phosphate tribasic and calcium dihydrogen phosphate was purchased from Ruibang Biomaterials Co., Ltd (Shanghai, China). Genex® composed of calcium sulfate and β-tricalcium phosphate was purchased from Biocomposites Ltd (Staffordshire, England).

2.2. Preparation of implants

PSC/CSCs were prepared via a combination of a solid phase and deionized water. The solid phase was prepared by mixing PSC particles and CSH powders with various PSC contents (10 w%, 30 w%, 50 w%, hereafter referred to as 10P/90C, 30P/70C, 50P/50C, respectively). Then, to obtain a homogeneous cement paste, the solid phase was mixed with deionized water for 30 s at a liquid-to-solid (L/S) ratio of 0.5 mL/g. Cement pastes were injected into Teflon moulds (Ø 6 mm × 10 mm). Then, they were removed from the moulds and air-dried at room temperature for 24 h.

CPC and Genex® were prepared in accordance with manufacturer's guidelines.

Before being used in *in vivo* and *in vitro* experiments, all samples were sterilized for 10 min by gamma radiation at 25 kGy.

2.3. Characterization

2.3.1. Setting time and injectability

Setting time for each sample (CSC, 10P/90C, 30P/70C and 50P/50C) was measured using a Vicat apparatus as previously reported [12]. Cement injectability was tested using a previously reported procedure [12]. Briefly, 4 g of the homogeneous cement paste was put into a 5 mL syringe. After adding water to the composite powders for 3 min, the cement was gently extruded by hand until it was too hard to push the syringe. Weight percentage of the cement that could be extruded from the syringe was used to evaluate injectability.

2.3.2. Structural and phase analyses

Microstructures of CSC, 10P/90C, 30P/70C and 50P/50C were evaluated by scanning electron microscopy (SEM; HITACHI, S4800, Japan). Their phase compositions were evaluated by X-ray diffraction (XRD; Bruker, Germany) using Cu Kα radiation at a scan rate of 3° min^{-1} within a 2θ range of 4°–60°.

2.3.3. Compressive strength

Compressive strength of CSC, 10P/90C, 30P/70C, 50P/50C, CPC and Genex® (Ø 6 mm × 10 mm) was evaluated using a computer controlled universal testing machine (AG-5kN, Shimadzu, Japan) with a crosshead speed of 0.5 mm/min until failure. Maximum stress before failure was defined as the compressive strength. In each group, three samples were tested to obtain the average compressive strength.

2.3.4. In vitro degradation

Degradation rates of CSC and PSC/CSCs were determined by monitoring weight-loss ratios of the samples [5]. Cements were soaked in absolute ethanol for 2 h and dried at 60 °C to a constant weight (M_0). Then, samples were immersed in Tris–HCl solution (pH 7.4) at a liquid to solid ratio of 20 mL/g and stored at 37.0 °C for different times (1, 2, 3 and 4 weeks). The Tris–HCl solution was refreshed once a week and the samples were obtained from the solution at the same time, gently rinsed using absolute ethanol and dried at 60 °C to a constant weight (M_t). Weight-loss ratio was calculated as: Weight loss = $(M_0 - M_t)/M_0 \times 100\%$. After soaking the cements for different times, ion concentration (Ca, P and Si) changes in the Tris–HCl solution were evaluated by inductively coupled plasma-atomic emission spectroscopy (ICP-AES, Varian 715 ES, California, USA).

2.4. Animal model

All animal studies were approved by Southern Medical University's Animal Care and Use Committee. All animal procedures were performed in accordance with the National Research Council's Guidelines for the Care and Use of Laboratory Animals. Three-month-old healthy male New Zealand rabbits (2.2–2.4 kg) were used in this study. A total of 45 rabbits were randomized into 10P/90C, 30P/70C, 50P/50C, CPC and Genex® groups. After anesthesia by intramuscular injection of Zoletil® 50 (0.1 mL/kg) mixed with Su-Mian-Xin II (0.1 mL/kg), critical sized defects (Ø 6 mm × 10 mm) were carefully made in femoral condyles using a medical drill [13]. Cylinders (Ø 6 mm × 10 mm) of 10P/90C, 30P/70C, 50P/50C, CPC and Genex® were respectively implanted into bilateral hind femoral condyles of nine rabbits in each group. The incision was sutured in a routine fashion. For Micro-CT studies and histological analyses, rabbits were sacrificed by air embolization at 4, 8 and 12 weeks postoperatively, for a total of 6 samples in each time group for each material group.

2.5. Micro-computed tomography

Micro-computed tomography (Micro-CT, Scanco Medical, μCT-80, Switzerland) was used to assess femoral condyle bone defects repair at 55 kV and 145 μA. The system has a camera (1024 × 1024 pixels) that acquires data by taking a number of planar images at regular angular intervals (36 μm). At each time point, 30 samples were obtained and micro-CT analyses performed. Then, the 3D images were reconstructed. Bone mineral density (BMD) and bone volume/total volume (BV/TV) fractions were quantified by a CT analysis software.

2.6. Histological assay

Fixed samples were decalcified in 5% ethylenediaminetetraacetic acid disodium salt (EDTA-2Na) solution (pH 7.2), paraffin-embedded, sliced into 5 μm thick sections using a microtome (Leica, Tokyo, Japan) and stained with haematoxylin and eosin (H&E) as well as Masson's trichrome stains (Sigma–Aldrich, USA), as instructed by the manufacturers. All sections were analyzed by bone histomorphometry under a semi-automated image analysis system.

Based on characterization, Micro-CT findings and histological analysis, the best formula of PSC/CSCs was selected, and compared to CPC and Genex® in subsequent experiments.

2.7. In vitro osteogenesis of PSC/CSC extracts

2.7.1. Cell culture and extract preparation

The MC3T3-E1 cells which purchased from the Cell Bank of the Chinese Academy of Sciences were used for osteogenesis analyses. Cells were cultured in α-Modified Eagle's Medium (α-MEM; Gibco, USA) with 10% fetal bovine serum (FBS; Gibco, USA) and 1% penicillin–streptomycin. Incubation was done in a 5% CO_2 atmosphere at 37 °C. After 3 to 6 passages, the MC3T3-E1 cells were used for subsequent cell experiments, and the culture medium refreshed every two days.

Extracts of selected PSC/CSC, CPC and Genex® were prepared as previously reported [14,15]. Briefly, at a mass to liquid volume ratio of 100 mg/mL, sterilized selected PSC/CSC, CPC and Genex® were separately soaked in α-MEM, and maintained in a shaker at 60 rpm and 37 °C. After 24 h of incubation, extracts were collected by centrifugation and detected by inductively coupled plasma-atomic emission spectroscopy to determine the ionic concentrations of calcium, phosphorus and silicon (Ca, P and Si). Changes in pH values of the extracts were measured by a pH test-meter (Denver UB-7, YaoHua Co, China). Thereafter, extracts were sterilized using a 0.22 μm filter membrane (Millipore, USA), after which 10% FBS, 1% penicillin–streptomycin, 10 mM β-glycerophosphate (Sigma, USA) and 50 μM ascorbic acid (Sigma, USA) were added to the extracts for further analyses.

2.7.2. Cell adhesion and proliferation assays

To assess cell adhesion, MC3T3-E1 cells were seeded on selected PSC/CSC, CPC and Genex® disks (Ø 10 mm × 2 mm) respectively in 24-well culture plates (1.0×10^5 cells/mL) containing α-MEM complete medium. Cell-seeded cements were incubated in an incubator and cultured for 24 h. Then, the medium was removed, after which samples were gently rinsed thrice with PBS and fixed in 2.5% glutaraldehyde [9]. The fixative was removed by washing with PBS followed by sequential dehydration in a series of graded ethanol ($V_{ethanol}/V_{distilled\ water}$ = 50, 70, 90, 95 and 100%). Morphologies of the attached cells were evaluated by SEM.

A Cell Counting Kit-8 (CCK-8; Dojindo, Japan) assay was performed to determine MC3T3-E1 cell proliferation. Briefly, MC3T3-E1 cells were seeded in a 96-well plate (3.1×10^4 cells/cm^2) and incubated for 12 h. Then, the culture medium was replaced with different extracts or osteogenic inductive medium (α-MEM plus 10% FBS, 1% penicillin–streptomycin, 10 mM β-glycerophosphate and 50 μM ascorbic acid) and further incubated for 24 h. The CCK-8 assay was performed as instructed by the manufacturer. Absorbance was spectrophotometrically determined at 450 nm. There were five parallel samples in each group.

2.7.3. Migration assay

Cell migration analysis was performed by a wound healing assay, as previously reported [16]. Briefly, MC3T3-E1 cells were seeded in a 12-well plate. At 90% cell confluence, a linear scratch was generated using a plastic pipette tip. Floating cells were removed using PBS after which the culture medium was separately replaced by extracts of selected PSC/CSC, CPC and Genex® or osteogenic inductive medium. Wound closure was imaged at indicated times by inverted microscopy (Olympus, Tokyo, Japan). The degree of scratch closure was evaluated by the Image J software.

2.7.4. Alkaline phosphatase staining assay

Alkaline phosphatase (ALP) staining was performed using a BCIP/NBT ALP kit (Beyotime, Shanghai, China). Briefly, MC3T3-E1 cells were plated in 12-well plates. Twelve hours later, the culture medium was separately replaced by extracts of selected PSC/CSC, CPC and Genex® or osteogenic inductive medium for 7 days. After fixation in 4% paraformaldehyde, cells were washed twice with PBS and incubated with ALP staining buffer for 20 min. ALP activity of each sample was determined from optical density (OD, 450 nm) values.

2.7.5. Alizarin red assay

Alizarin red staining was performed to assess the extracellular matrix calcification of MC3T3-E1 cells. Briefly, MC3T3-E1 cells were seeded and cultured in 12-well plates with extracts of selected PSC/CSC, CPC and Genex® or osteogenic inductive medium for 21 days. Thereafter, cells were fixed in 4% paraformaldehyde for 15 min, and stained with 1% (w/v) Alizarin Red dye (pH 4.1–4.5) (Sigma–Aldrich, USA) for 60 min at room temperature.

After imaging by inverted microscopy, the stain was desorbed with 10% (w/v) cetylpyridinium chloride (Sigma–Aldrich, USA) and the absorbance of the extract solution determined using a microplate reader (BioTek, Winooski, VT, USA) at 562 nm for quantification.

2.7.6. qRT-PCR gene expression assays

Total cellular RNA was extracted as previously described [17,18]. Briefly, after cultured with different extracts or osteogenic inductive medium for 14 days, total RNA was isolated from treated MC3T3-E1 cells using a TRIzol Reagent (Life Technologies, USA), as instructed by the manufacturer. Then, RNA content was detected by Nanodrop 2000 (Thermo Scientific, USA). The isolated RNA was reverse transcribed into complementary DNA (cDNA) using the iScript cDNA Synthesis Kit (Roche SR, USA). Then, quantitative real-time polymerase chain reaction was performed using the SYBR Premix ExTaq II kit (Life Technologies, USA) on a LightCycler 96 Real-Time PCR system (Roche, Basel, Switzerland). Gene expressions were calculated by the $2^{-\Delta\Delta Ct}$ method. Primer sequences used in this assay are shown in Table 1.

2.7.7. Western blot analysis

Western blot analysis was performed to assess Runx2, Col I and OCN protein expressions, as previously described [19]. After cultured in different extracts or osteogenic inductive medium for 14 days, MC3T3-E1 cells were lysed for 30 min using an ice-cold lysis buffer containing 1 mM phenylmethylsulphonyl fluoride (PMSF) (Sigma, USA) and phosphatase inhibitor cocktail (Sigma, USA). Then, cell lysates were loaded onto SDS-polyacrylamide gels and transferred to nitrocellulose (NC) membranes (Amersham Biosciences, USA). Membranes were incubated overnight at 4 °C with primary antibodies: Runx2 (1:1000, ab76956, Abcam), Col I (1:3000, ab34710, Abcam), OCN (1:2000, ab13420, Abcam), and β-actin (1:1000, ab8227, Abcam). Then, they were washed thrice using the Tris-buffered saline (TBS) containing 0.05% Tween-20 (TBST) followed by 60 min of incubation with appropriate horseradish peroxidase-conjugated secondary antibodies. An enhanced

Table 1
Sequences of primers used for qRT-PCR.

Genes	Primers	Sequences (5′-3′)
Runx2	Forward	CCGTGGCCTTCAAGGTTGT
	Reverse	TTCATAACAGCGGAGGCATTT
Col I	Forward	GCTCCTCTTAGGGGCCACT
	Reverse	CCACGTCTCACCATTGGGG
OCN	Forward	CTTGAAGACCGCCTACAAAC
	Reverse	GCTGCTGTGACATCCATAC
β-Actin	Forward	CTGACTGACTACCTC
	Reverse	GACAGCGAGGCCAGGATG

chemiluminescence system (Syngene, Cambridge, UK) was used to determine chemiluminescence.

2.8. In vitro angiogenesis of PSC/CSC extracts

2.8.1. Cell culture and extract preparation

Human umbilical vein endothelial cells (HUVECs) which purchased from the Cell Bank of the Chinese Academy of Sciences were used to assess the angiogenesis potential of selected PSC/CSC, CPC and Genex® extracts. High-glucose Dulbecco's Modified Eagle's Medium (H-DMEM; Gibco, USA) supplemented with 10% FBS and 1% penicillin–streptomycin solution was used for culturing the HUVECs. After 3 to 6 passages, HUVECs were used for subsequent cell experiments, and the culture medium refreshed every two days.

At a mass to liquid volume ratio of 100 mg/mL, the selected PSC/CSC, CPC and Genex® were separately soaked in H-DMEM, and maintained in a shaker at 37 °C, 60 rpm for 24 h. Then, extracts were collected by centrifugation and the supernatants sterilized via a 0.22 μm filter membrane. Thereafter, extracts were supplemented with 10% FBS and 1% penicillin–streptomycin, and stored at 4 °C for subsequent analyses.

2.8.2. Cell adhesion and proliferation assays

HUVECs were seeded on different cement disks (selected PSC/CSC, CPC and Genex®) (Ø 10 mm × 2 mm) placed in 24-well plates to assess cell adhesion. Cells were cultured in H-DMEM complete medium and incubated for 24 h. Then, cell attachment of HUVECs on cement disks were characterized by SEM as described in the "*In vitro* osteogenesis of PSC/CSC extracts" section.

To evaluate the effects of different extracts on proliferation of HUVECs, the CCK-8 assay was performed. Briefly, HUVECs were seeded in a 96-well plate and incubated for 12 h. Then, the H-DMEM complete medium was replaced by different extracts, and incubation continued for 24 h. Only H-DMEM complete medium cultured HUVECs were considered as the control group. Then, the CCK-8 assay was performed as described in the "*In vitro* osteogenesis of PSC/CSC extracts" section.

2.8.3. In vitro angiogenesis assay

Effects of cement extracts on vascular tube formation of HUVECs were assessed using the Matrigel® Matrix (Corning Inc., USA). Briefly, a 96-well plate was covered by a polymerized Matrigel layer prior to HUVECs seeding. HUVECs were separately seeded (2×10^4 cells/well) on the polymerized Matrigel in the presence of the extracts of selected PSC/CSC, CPC and Genex®. The HUVECs that had been cultured on Matrigel without extracts were considered the control group.

After incubation at 37 °C for 6 h, tube formation was assessed by inverted microscopy, and five microscopic areas were randomly selected for imaging. The total branching length and number of branches were quantified by imaging analysis.

2.9. Statistical analysis

Data are expressed as mean ± standard deviation (SD). Differences in means among groups were measured by one-way ANOVA. All statistical analyses were performed using the SPSS 22.0 software (IBM, Armonk, NY, USA). $P < 0.05$ was the threshold for significance.

3. Results

3.1. Characterization of bone cements

The addition of PSC prolonged the initial and final setting times of bone cements (Fig. 1A). When 30% PSC was added into CSC, the initial setting time was prolonged from 4.0 to 7.8 min while the final setting time was extended from 8.5 to 13.5 min. When the mass ratio of PSC reached 50%, the initial and final setting times were increased to 18.7 and 27.7 min, respectively. Injectability of the cements decreased with increasing PSC content (Fig. 1B). After setting for 3 min, CSC and 10P/90C were completely injected (96% and 95%), while injectable amounts of 30P/70C and 50P/50C dropped to 93% and 85%, respectively. In addition, slight phase separation was observed in the 50P/50C group.

Fig. 2A shows SEM images of CSC and PSC/CSCs. The CSC consists of rod-like crystals (Fig. 2A1) while PSC consists of irregular aggregates of tiny particles. The rod-like CSC and irregular PSC aggregates could both be observed in PSC/CSCs, in which PSC particles were distributed within interstices between CSC crystals. With increasing PSC content, the amounts of tiny particles increased, as expected (Fig. 2A2, A3 and A4).

When PSC/CSC powders were mixed with water, the main product of the hydration process was calcium sulfate dihydrate (CSD). The PSC phase could be clearly observed for 30P/70C and 50P/50C, but were not so clear for 10P/90C in XRD patterns (Fig. 2B).

Compressive strength of the cements is shown in Fig. 2C. Compressive strength of 10P/90C (4.2 ± 0.1 MPa) and 30P/70C (3.5 ± 0.3 MPa) was higher than those of CSC (3.2 ± 0.2 MPa), while the compressive strength of 50P/50C (0.6 ± 0.1 MPa) was markedly lower than that of CSC ($p < 0.05$). The compressive strength of CPC reached 8.1 ± 0.5 MPa, which was higher than that of Genex® (1.3 ± 0.1 MPa) and 30P/70C.

Fig. 3A shows cement degradation after soaking in Tris–HCl solution for different time periods (1, 2, 3 and 4 weeks). All cements exhibited a sustained weight loss with increasing soaking time. After soaking for 4 weeks, weight loss of CSC (approximately 25 w%) was lower than those of 30P/70C (approximately 32 w%) and 50P/50C (approximately 38 w %). Fig. 3B, C and D shows changes in Ca, P and Si ion concentrations in Tris–HCl solutions after soaking the cements for different times. Levels of released Ca ions at different time points were comparable for all groups. Cements with higher PSC contents released higher amounts of P and Si into the Tris–HCl solution. Meanwhile, the amounts of released P and Si in the same group at different time points were relatively stable.

3.2. In vivo bone defect repair

3.2.1. Micro-CT images

Micro-CT images show that positions of cements in femoral condyles were similar for all animals (Fig. 4A). Sagittal images and 3D reconstruction images of the newly formed bone tissues at the defects were used for evaluation of *in vivo* osteogenic capacity of the cements. In the 10P/90C group, the bone cement was rapidly almost completely absorbed at 8 weeks, meanwhile, only a small amount of bone tissue was formed at the edge of the defect after 12 weeks. Similarly, in the Genex® group, the bone cement degraded very fast. More than half of the cement had degraded at 8 weeks and completely degraded before 12 weeks. Although there was new bone tissue formation around the defect at 12 weeks, the defect void in the center was still obvious. In the 30P/70C group, from 4 weeks to 12 weeks, the cement degraded slowly with gradual ingrowth of the bone tissue. After 12 weeks, the cement seemed to have been completely degraded, and bone trabecular had almost completely filled the bone defect, achieving a good balance between degradation and bone regeneration. The 50P/50C group showed that the bone cement had degraded slower than 30P/70C, and after 12 weeks, there was still a large amount of bone cement left, although partially replaced by new bone tissues. Regarding the CPC group, from 4 weeks to 12 weeks, the bone cement showed little changes and only a few newly formed bones appeared at the bone-cement interface.

BMD and BV/TV fractions within the defects were calculated to evaluate bone growth at 12 weeks (Fig. 4B and C, respectively). The BMD of 30P/70C (603.6 ± 30.5 mg/cm^3) was much higher than those of 10P/90C (248.1 ± 13.7 mg/cm^3), 50P/50C (417.3 ± 20.2 mg/cm^3), CPC (81.8 ± 12.2 mg/cm^3) and Genex® (401.7 ± 20.0 mg/cm^3). Meanwhile, BV/TV of 30P/70C (39.5 ± 3.5%) was significantly higher ($p < 0.05$) than those of 10P/90C (21.8 ± 1.4%), 50P/50C (27.8 ± 2.6%), CPC (4.8 ± 1.7%) and Genex® (23.7 ± 2.0%).

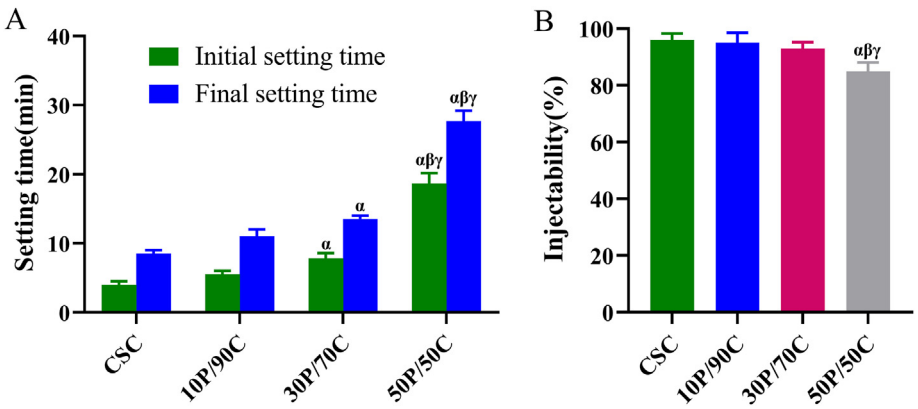

Fig. 1. Setting time (A) and injectability (B) of different cements (CSC, 10P/90C, 30P/70C and 50P/50C). Significantly different ($p < 0.05$): α, from CSC group; β, from 10P/90C group; γ, from 30P/70C group.

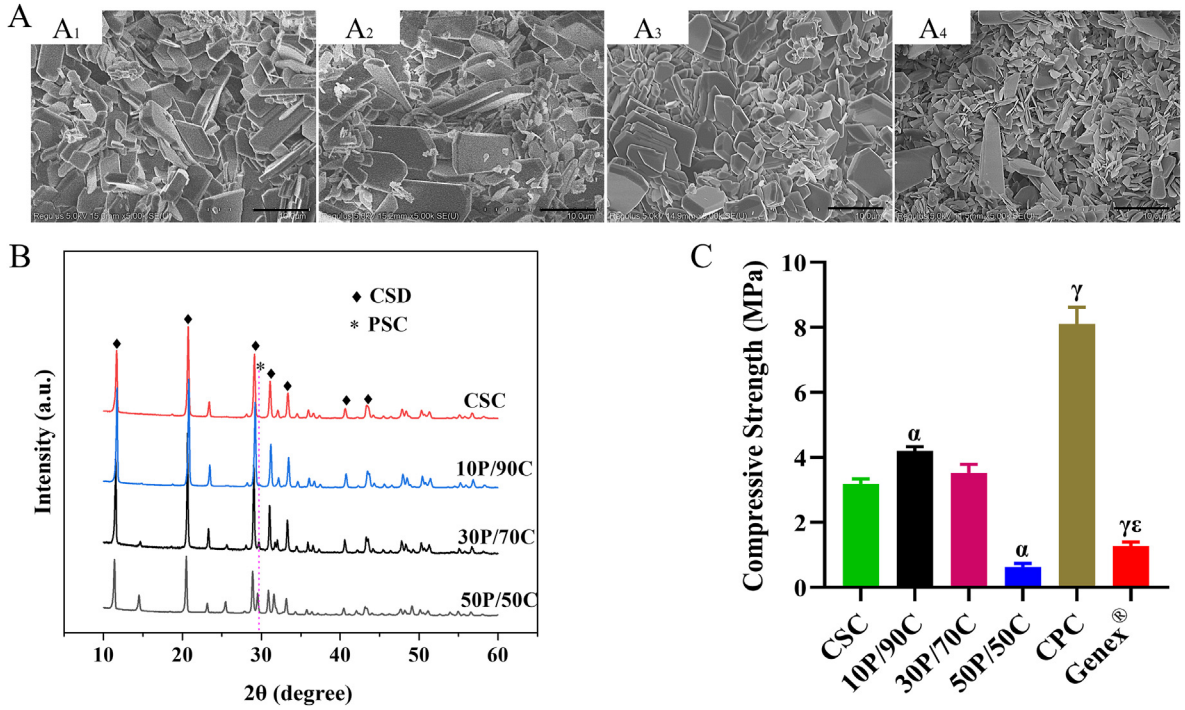

Fig. 2. (A) SEM images of CSC (A1), 10P/90C (A2), 30P/70C (A3) and 50P/50C (A4). Scale bar: 5 μm (B) XRD patterns of CSC, 10P/90C, 30P/70C and 50P/50C. (C) Compressive strength of cements (CSC, 10P/90C, 30P/70C, 50P/50C, CPC and Genex®). Significantly different ($p < 0.05$): α, from CSC group; γ, from 30P/70C group; ε, from CPC group.

3.2.2. *Histological assay*

Consistent with Micro-CT findings, images of H&E and Masson's trichrome staining are shown in Fig. 5. In 10P/90C and Genex® groups, the newly formed thin trabeculae could be seen at the edge of the bone defects, however, the defects were still obvious. The number of new bone trabeculae was similar in both groups. In the 30P/70C group, the bone defect area was almost completely filled with the bone tissue, however, a small amount of material (presumably PSC) remained between the bone trabeculae. Numerous neovascularization could also be seen in H&E staining. In the 50P/50C group, numerous new bone trabeculae and abundant residual material (presumably PSC) were seen at the edge of the defect, and the central cavity of the defect was still evident. In the CPC group, the bone-cement interface was smooth and there was almost very little bone tissue ingrowth.

The above findings show that 30P/70C was the best formulation of PSC/CSCs. It had a suitable operability, compressive strength and bone regeneration ability. Thus, 30P/70C was chosen for further investigation *in vitro*, with conventional cements (CPC and Genex®) as controls.

3.3. *Ionic concentrations and pH values of the extracts*

Ionic concentrations and pH values of different extracts are shown in Table 2. The Ca, P and Si contents in the CPC group were almost the same as those in α-MEM. Compared to α-MEM, Genex® and 30P/70C released much higher amounts of Ca ions into the media during the immersion period. In contrast, P amounts in α-MEM were much higher than those in the 30P/70C group. However, Si ion concentrations in the 30P/70C group (approximately 7.2 mg/L) were higher than those in α-MEM, CPC and Genex® groups. The pH value of the 30P/70C group was approximately 7.30, which was slightly higher than those for the α-MEM (approximately 7.25) and CPC (approximately 7.26) groups.

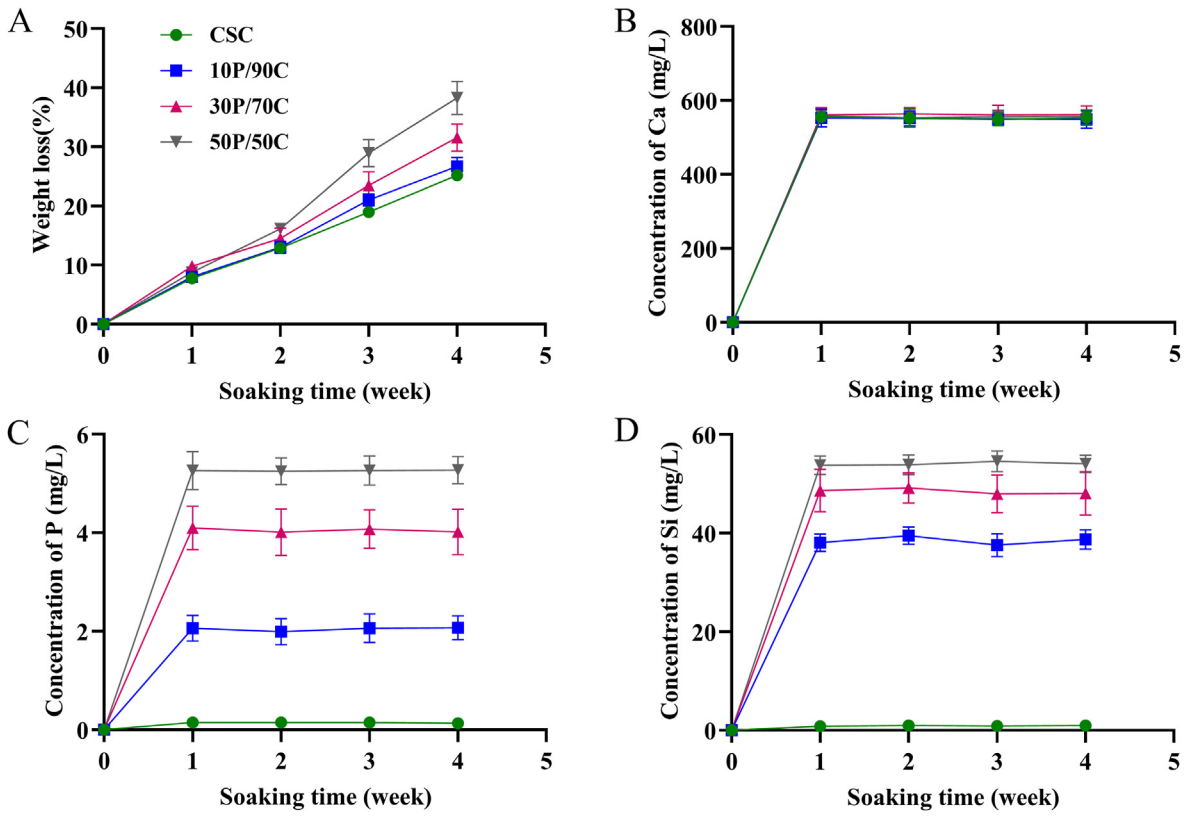

Fig. 3. (A) Weight loss and (B–D) Ca, P and Si ion concentration changes of Tris–HCl solution after soaking different cements (CSC, 10P/90C, 30P/70C and 50P/50C) for different times (1, 2, 3 and 4 weeks).

3.4. Adhesion of MC3T3-E1 cells cultured on cements

MC3T3-E1 cell attachment and morphology on CPC, Genex® and 30P/70C disks were evaluated by SEM (Fig. 6). After 24 h of incubation, all cements supported MC3T3-E1 cell attachment and cells elongated on the CPC and Genex® surfaces with several cytoplasmic digitations. In contrast, cells spread well on the surface of 30P/70C, exhibiting a flattened appearance with lamellipodia adhered to the cement.

3.5. Effects of 30P/70C, CPC and Genex® extracts on MC3T3-E1 cell proliferation and migration

A CCK-8 assay was performed to determine cell proliferation. As shown in Fig. 7A, MC3T3-E1 cell proliferation in groups with 30P/70C and Genex® extracts was significantly higher ($p < 0.05$) than that of CPC and control groups. Meanwhile, proliferation was higher in the 30P/70C group, relative to the Genex® group ($p < 0.05$), indicating better biological activities of 30P/70C.

MC3T3-E1 cells were treated with CPC, Genex® and 30P/70C extracts for 12 h to assess their migration capacity. The osteogenic inductive medium was used as the control group. As shown in Fig. 7B and C, 30P/70C and Genex® groups significantly promoted MC3T3-E1 cell migration, compared to CPC and control groups ($p < 0.05$). Differences in migration capacity between the CPC and control groups were insignificant. The 30P/70C group was better at promoting the migration of MC3T3-E1 cells, relative to the other three groups.

3.6. Effects of 30P/70C, CPC and Genex® extracts on osteogenic differentiation of MC3T3-E1 cells

Compared to control and CPC groups, the 30P/70C and Genex® groups exhibited significantly higher ALP activity ($p < 0.05$), especially the 30P/70C group. Differences in ALP activity between CPC and control groups were insignificant (Fig. 8A and B).

Alizarin red staining and quantification showed that 30P/70C and Genex® groups were much better than the CPC and control groups, and differences between the 30P/70C and Genex® groups were marked ($p < 0.05$). Mineralized nodules were most obvious in the 30P/70C group (Fig. 8C and D).

After treated with CPC, Genex® and 30P/70C extracts for 14 days, the transcription profile of a panel of osteoblast markers in MC3T3-E1 cells was determined by qRT-PCR (Fig. 9A, B and C, respectively). In the presence of 30P/70C extracts, MC3T3-E1 cells exhibited a marked increase in Runx2, Col I and OCN mRNA levels. In addition, a significant upregulation ($p < 0.05$) was observed in the Genex® group, compared to CPC and control groups.

Western blot assay was also performed to determine whether 30P/70C extracts could promote osteogenic protein expressions. Runx2, Col I and OCN levels in 30P/70C and Genex® groups were higher than those in CPC and control groups, and 30P/70C was still the highest (Fig. 9D).

These results indicate that compared to CPC and Genex® extracts, 30P/70C extracts significantly promoted the osteogenic differentiation of MC3T3-E1 cells.

3.7. Adhesion of HUVECs cultured on cements

To reveal cell adhesion to surfaces of different cements (CPC, Genex® and 30P/70C, respectively), SEM observation of HUVECs cultured on cement disks was performed at 24 h after seeding. As shown in Fig. 10, all cement groups supported HUVECs attachment. The cells showed spindle-like or triangular morphologies and had close contacts with cements. The results indicate that all cements had no negative effects on cell morphologies.

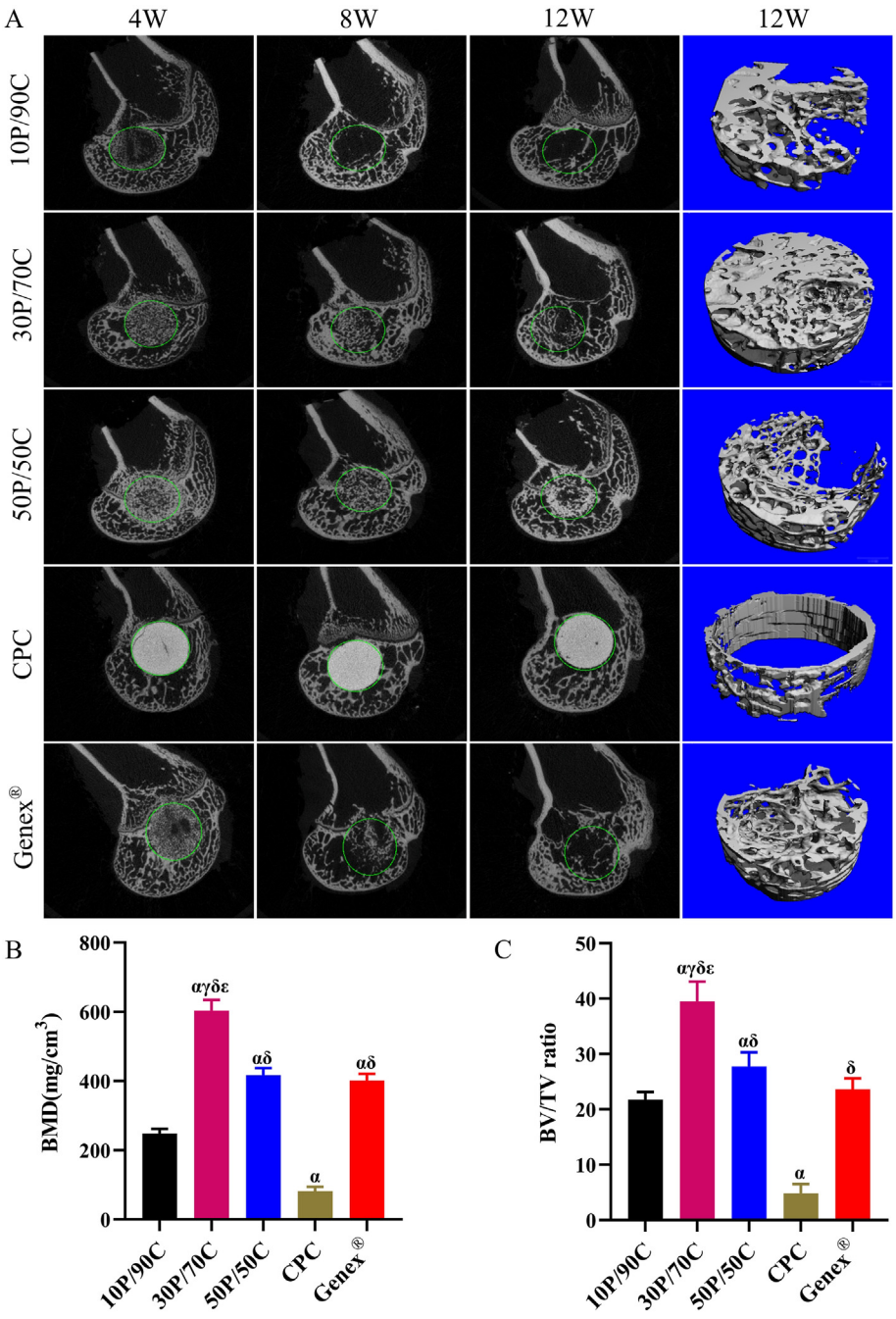

Fig. 4. Micro-CT image analysis of bone regeneration of rabbit femoral condyle bone defects repaired with different cements (10P/90C, 30P/70C, 50P/50C, CPC and Genex®). (A) Sagittal images (4, 8 and 12 weeks) of bone formation ability; 3D reconstruction images (12 weeks) of bone formation ability. Diameter of the circle is 6 mm. (B) Statistical analysis of bone mineral density (BMD) in the defect area at week 12. (C) Statistical analysis of bone volume/total volume (BV/TV) fraction in the defect area at week 12. Significantly different ($p < 0.05$): α, from 10P/90C group; γ, from 50P/50C group; δ, from CPC group; ε, from Genex® group.

3.8. Effects of 30P/70C, CPC and Genex® extracts on proliferation of HUVECs

Viability of HUVECs that had been respectively cultured in CPC, Genex® and 30P/70C extracts for 24 h is shown in Fig. 11A. Cell viability in the 30P/70C group was significantly higher than that in other groups ($p < 0.05$). Genex® and CPC groups exhibited higher cell viability, relative to the control group, however, differences were insignificant.

3.9. In vitro angiogenesis assay

An *in vitro* Matrigel® Matrix was used to assess the angiogenic capacity of different extracts. As shown in Fig. 11B, C and D, after incubation for 6 h either in the presence or absence of extracts, all the HUVECs that had been cultured on Matrigel® Matrix gradually assembled to form branches. However, the 30P/70C extracts were able to induce a significant increase in total branching length and number of branches, compared to other groups ($p < 0.05$).

4. Discussion

As bone augmentation materials, bone cements form a class of the most promising choices. Good mechanical performance is of great importance because it allows the cements to maintain their space, withstand external forces, and avoid stress shielding [20,21]. Ideally, once implanted, the cements should be able to provide the required mechanical support to share the load with the surrounding bone tissues. In this study, with incorporation of PSC, the compressive strength of CSC increased from 3.2 ± 0.2 MPa to 4.2 ± 0.1 MPa (10P/90C) and 3.5 ± 0.3 MPa (30P/70C). However, the compressive strength of 50P/50C (0.6 ±

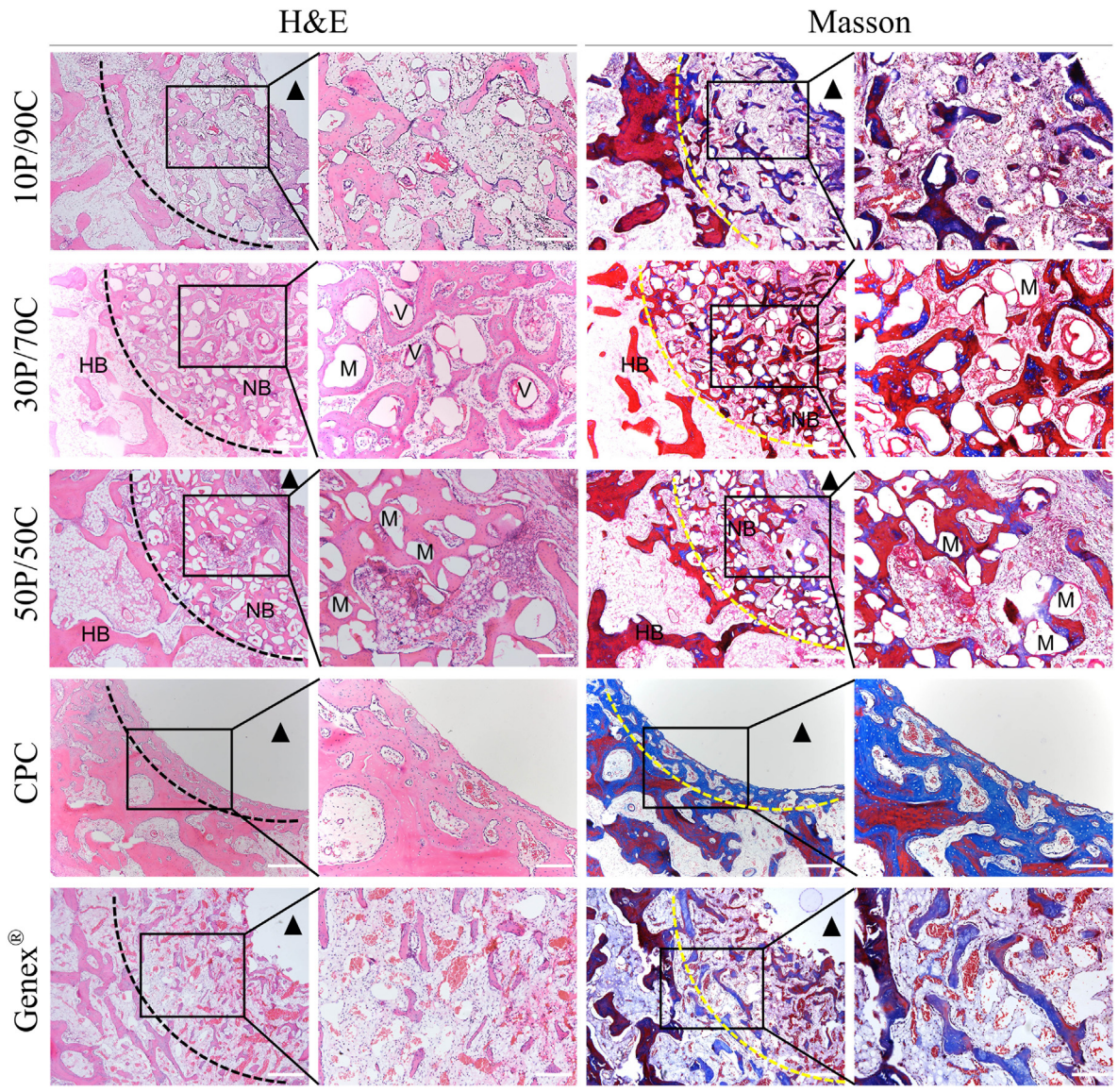

Fig. 5. Histological observation (H&E and Masson's trichrome staining) of the rabbit femoral condyle bone defects repaired with different cements (10P/90C, 30P/70C, 50P/50C, CPC and Genex®) 12 weeks after surgery (HB: host bone, NB: nascent bone, V: blood vessel, M: material. Black or yellow dotted line denotes the bone defect site. The black triangle indicates the unhealed central bone cavity). Scale bar: 500 μm (low magnification) and 200 μm (high magnification).

Table 2
Ionic concentrations (mean ± SD) (mg/L) and pH values of different extracts.

	Ca	P	Si	pH
α-MEM	45.8 ± 0.7	31.4 ± 0.6	<1.0	7.25 ± 0.045
CPC	48.5 ± 0.9	35.2 ± 0.8	<1.0	7.26 ± 0.031
Genex®	64.1 ± 1.1	38.5 ± 0.8	<1.0	7.21 ± 0.023
30P/70C	92.0 ± 1.2	15.3 ± 0.7	7.2 ± 1.3	7.30 ± 0.034

0.1 MPa) was much lower than that of CSC (Fig. 2C). Therefore, addition of certain proportions of PSC enhances the compressive strength of CSC, while a large amount of PSC is unfavorable to the mechanical strength of PSC/CSC. This may be because the inclusion of excess non-curing PSC induced a reduction in strength. The compressive strength of hardened 30P/70C fulfills the requirements for cancellous bone substitutes [22, 23].

We also established the osteogenic potential of 30P/70C *in vivo* and *in vitro*. *In vivo*, 30P/70C had a good efficacy for bone defect repair. Micro-CT and histological analyses showed that the 30P/70C formula promoted bone tissue regeneration better than the other two formulations. Compared to CPC and Genex®, 30P/70C stimulated more new bone formation much earlier and more extensively in the defect area throughout the whole investigation period (Figs. 4 and 5), suggesting that 30P/70C served as a favorable cement to enhance bone regeneration. Previous studies reported that Si ions promote osteoblast proliferation and differentiation [24–27]. Hence, superior bone regeneration is thought to be stimulated by bioactive ions (Si) released from 30P/70C at the location of bone defects, which promote cell proliferation and differentiation. We postulated that the outstanding bone regeneration performance might be partially related to suitable degradation. Specifically, rapid degradation (10P/90C and Genex®) might lead to the loss of osteoconductivity in the early stages of bone repair while slow degradation (CPC and 50P/50C) impeded the ingrowth of new bone tissues.

In vitro, osteogenic differentiation is a gradual process that is characterized by transient gene expression, and microenvironmental changes can lead to gene expression [19]. In this study, Runx2 mRNA levels were significantly enhanced by 30P/70C extracts, indicating early stages of osteogenic induction (Fig. 9A). Meanwhile, a marked increase in Col I and OCN mRNA levels was also observed on day 14, implying the onset of extracellular calcium deposition (Fig. 9B and C). ALP activity and

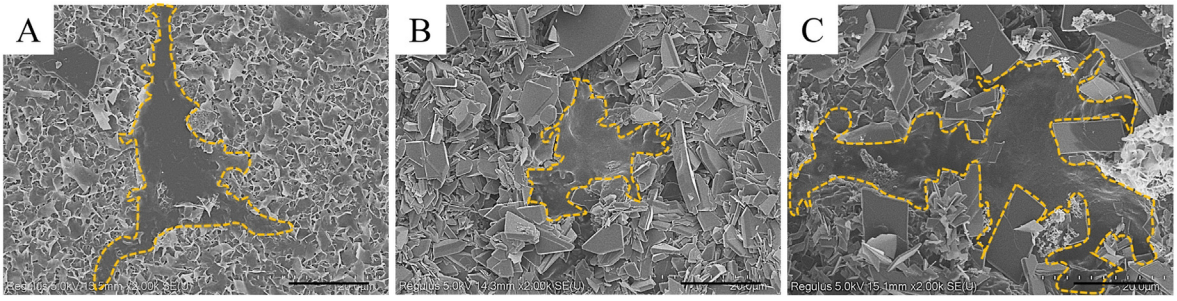

Fig. 6. At 24 h after seeding, SEM micrographs of MC3T3-E1 cells on CPC (A), Genex® (B) and 30P/70C (C). Scale bar: 10 μm.

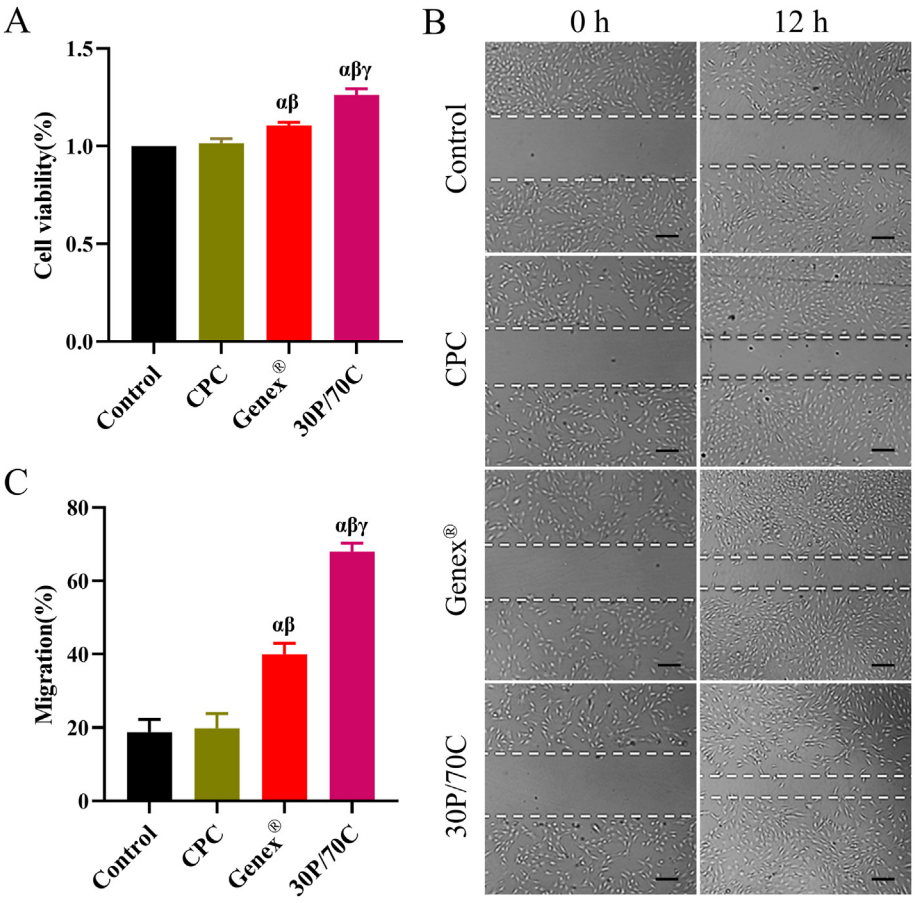

Fig. 7. Effects of different extracts (extracts of CPC, Genex® and 30P/70C) on MC3T3-E1 cells proliferation and migration processes. (A) CCK-8 assay results revealed the effects of different cement extracts on MC3T3-E1 cell proliferation. (B) Migration assay of MC3T3-E1 cells treated with extracts of different cements at 12 h. Scale bar: 50 μm. (C) Mean percentage of wound closure. Significantly different ($p < 0.05$): α, from Control group; β, from CPC group; γ, from Genex® group. Cells cultured in the osteogenic inductive medium were set as the control group.

western blot assays showed that ALP, Runx2, Col I and OCN protein levels were significantly increased by 30P/70C extracts, compared to those of CPC and Genex® (Fig. 8A and B, Fig. 9D, respectively). Alizarin red staining revealed more mineralized nodules in the 30P/70C group, relative to other experimental and control groups (Fig. 8C and D). These experimental results prove that MC3T3-E1 cells cultured with 30P/70C extracts differentiated towards the osteogenic lineage faster than cells cultured with CPC and Genex® extracts. Ionic products (Si and Ca) from BG have been shown to promote osteoblast proliferation and differentiation [28,29]. We found that Si and Ca ion concentrations of 30P/70C extracts were much higher than those of CPC and Genex® extracts (Table 2). Therefore, we deduced that it might be the Si and Ca ions released by 30P/70C during the degradation process that resulted in better osteogenic differentiation performances. Ca and P ions have also been reported to promote osteoblast differentiation [30,31]. This explains why Genex® promoted the osteogenic differentiation of MC3T3-E1 cells in this study. However, it seemed that CPC extracts could not promote the osteogenic differentiation of MC3T3-E1 cells, which maybe because CPC was hard to degrade, therefore, the amounts of Ca and P ions released by CPC were too small to play osteogenic roles. These results indicate the importance of bone cement composition in bone regeneration.

Angiogenesis is a pivotal step in new bone formation, and it is necessary for blood supply and facilitating subsequent osteogenesis [17,32]. Several approaches have been proposed to promote angiogenesis, including delivery of potential angiogenic inducible factors and prevascularization [33–36]. However, angiogenic induction by biomaterials could be a simple and effective neovascularization method [15]. In the *in vitro* study, the Matrigel® Matrix was used as the *in vitro* angiogenic model. We established that the 30P/70C extracts were able to induce a visible increase in total branching length and number of branches (Fig. 11B, C and D). Moreover, the 30P/70C extracts stimulated HUVECs proliferation (Fig. 11A). Taken together, 30P/70C extracts had stimulatory effects on angiogenesis. This may also explain the suitable bone

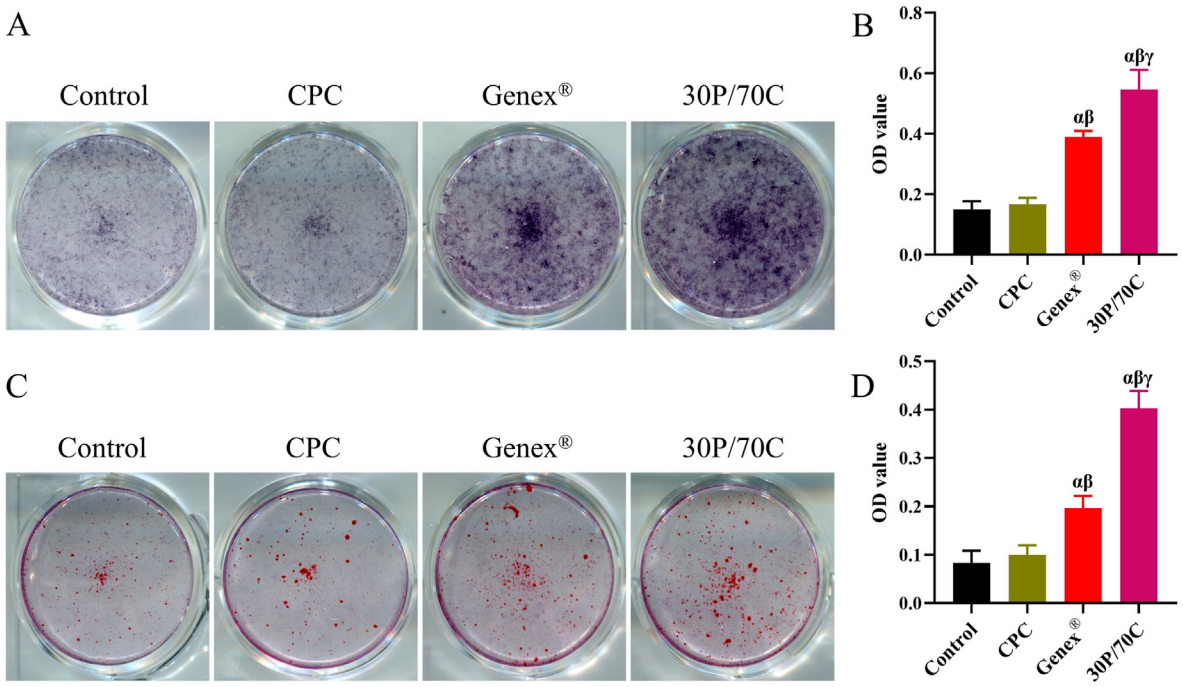

Fig. 8. ALP staining and Alizarin red staining of MC3T3-E1 cells cultured with different cement extracts (extracts of CPC, Genex® and 30P/70C). (A) ALP staining of early osteogenic differentiation of MC3T3-E1 cells on day 7. (B) The mean OD value of ALP staining in each group. (C) Alizarin red staining of mineralized MC3T3-E1 cells on day 14. (D) The mean OD value of Alizarin red staining in each group. Significantly different ($p < 0.05$): α, from Control group; β, from CPC group; γ, from Genex® group. Cells cultured in the osteogenic inductive medium were set as the control group.

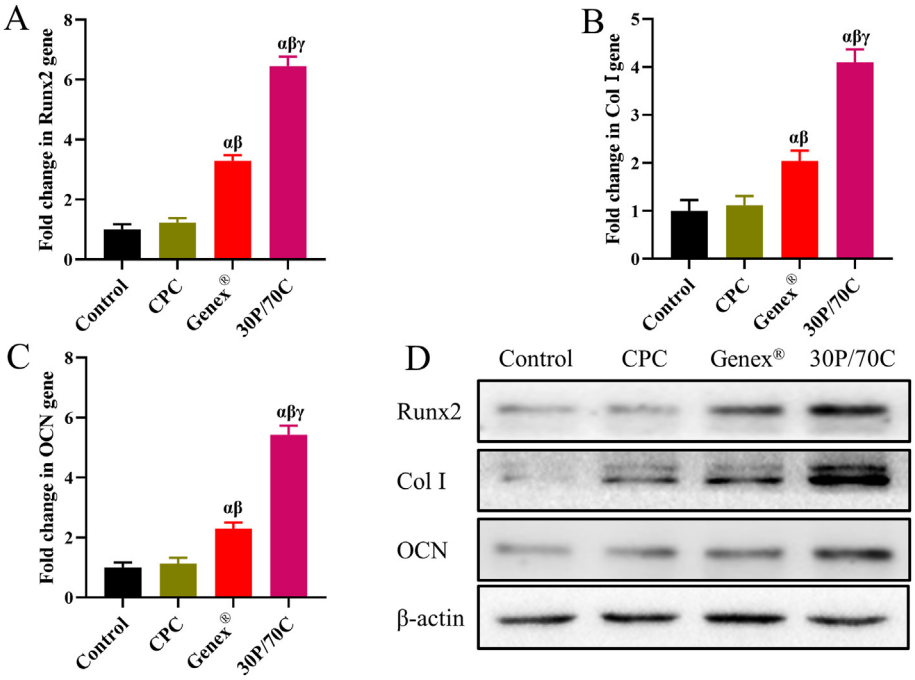

Fig. 9. Effects of different cement extracts (extracts of CPC, Genex® and 30P/70C) on osteogenic differentiation of MC3T3-E1 cells. (A–C) qRT-PCR analysis of osteogenesis-specific genes in MC3T3-E1 cells cultured in different extracts for 14 days. (D) Expression profiles of key proteins in MC3T3-E1 cells cultured in different extracts for 14 days. Significantly different ($p < 0.05$): α, from Control group; β, from CPC group; γ, from Genex® group. Cells cultured in the osteogenic inductive medium were set as the control group.

regeneration ability of 30P/70C *in vivo*. Zhai et al. showed that a silicate based bioceramic could stimulate angiogenesis [15]. Zhang et al. reported that Si ions released from a silicate based bioceramic scaffold were key in enhancing angiogenesis [37]. When added into other biomaterials, Si ions are also beneficial for angiogenesis [38–40]. We presumed that it could be the Si ions released from 30P/70C that played a pivotal role in stimulation of angiogenesis. These findings suggest that the use of BG based composite cements for accelerating angiogenesis is a promising strategy.

5. Conclusions

In the present study, we proved the advantageous of combining the physicochemical properties and biological performance of PSC and CSH, and a series of novel injectable and bioactive PSC-based cements were developed. Among them, 30P/70C was identified as the best formula, because of its suitable operability, physical compressive strength and good *in vivo* bone regeneration ability. Meanwhile, compared to CPC and Genex®, 30P/70C also showed significantly increased new bone

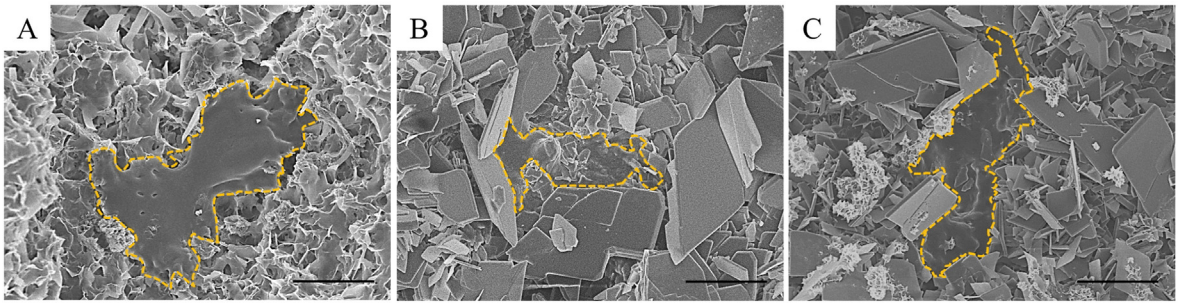

Fig. 10. At 24 h after seeding, SEM micrographs of adhesion of HUVECs on CPC (A), Genex® (B) and 30P/70C (C). Scale bar: 10 μm.

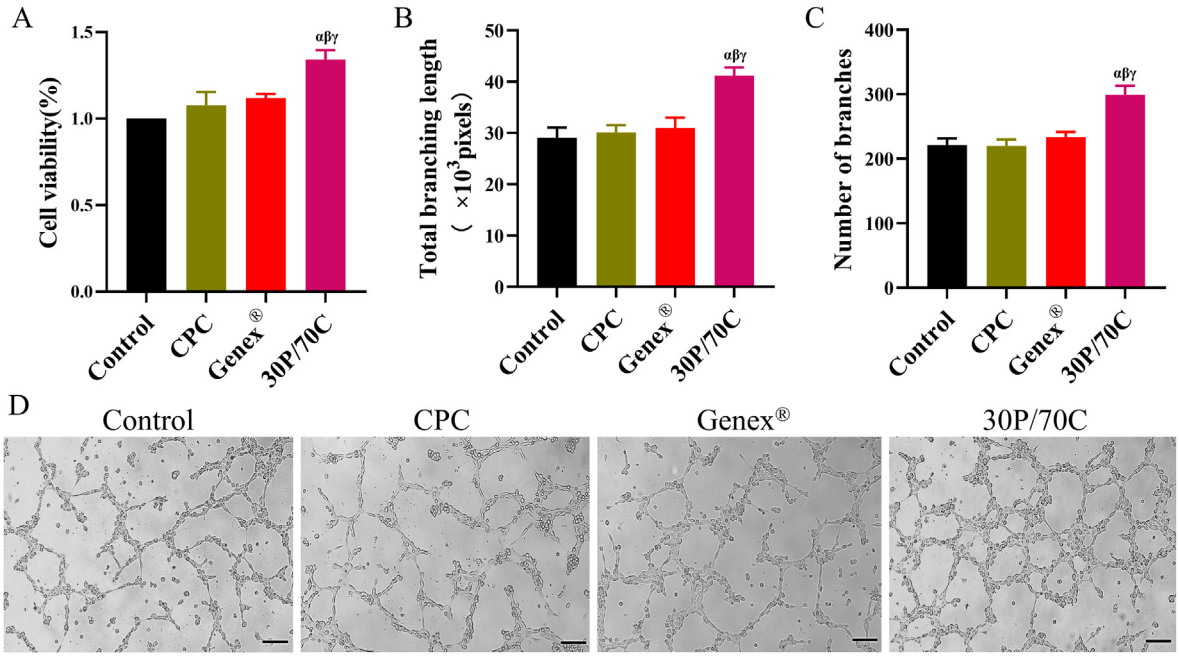

Fig. 11. Cell proliferation and tube formation assay of HUVECs cultured in different extracts (extracts of CPC, Genex® and 30P/70C). (A) Cell proliferation of HUVECs cultured in different extracts for 24 h. (B–D) Tube formation assay of HUVECs cultured on Matrigel® Matrix in the presence of different cement extracts for 6 h. (B, C) The statistics of total branching length and number of branches. (D) Optical images. Scale bar: 200 μm. Significantly different ($p < 0.05$): α, from Control group; β, from CPC group; γ, from Genex® group. Cells cultured in H-DMEM were set as the control group.

formation capacity in critical sized bone defects. *In vitro*, 30P/70C extracts promoted the osteogenic differentiation of MC3T3-E1 cells and enhanced the angiogenesis of HUVECs. These findings suggest that 30P/70C is an injectable pH neutral BG-based bone cement that may open up new opportunities for rapid repair of critical sized bone defects.

Funding

This work was supported by the National Natural Science Foundation of China (No. 81874013, 81702199 and 31801012).

Declaration of competing interest

The authors have no conflicts of interest to disclose.

Acknowledgements

All persons who have made substantial contributions to the work reported in the manuscript (e.g., technical help, writing and editing assistance, general support), but who do not meet the criteria for authorship, are named in the Acknowledgements and have given us their written permission to be named. If we have not included an Acknowledgements, then that indicates that we have not received substantial contributions from non-authors.

Appendix A. Supplementary data

Supplementary data to this article can be found online at https://doi.org/10.1016/j.jot.2022.05.011.

References

[1] Sun H, Ma X, Li Z, Liu J, Wang W, Qi X. Release characteristics of enoxaparin sodium-loaded polymethylmethacrylate bone cement. J Orthop Surg Res 2021;16(1):108.
[2] Zhang L, Lu C, Lv Y, Wang X, Guo S, Zhang H. Three-Dimensional printing-assisted masquelet technique in the treatment of calcaneal defects. Orthop Surg 2021;13(3):876–83.
[3] Thomas MV, Puleo DA. Calcium sulfate: properties and clinical applications. J Biomed Mater Res B Appl Biomater 2009;88(2):597–610.
[4] Beuerlein MJ, McKee MD. Calcium sulfates: what is the evidence? J Orthop Trauma 2010;24(Suppl 1):S46–51.
[5] Lin M, Zhang L, Wang J, Chen X, Yang X, Cui W, et al. Novel highly bioactive and biodegradable gypsum/calcium silicate composite bone cements: from physicochemical characteristics to in vivo aspects. J Mater Chem B 2014;2(14):2030–8.
[6] Wei S, Ma JX, Xu L, Gu XS, Ma XL. Biodegradable materials for bone defect repair. Mil Med Res 2020;7(1):54.

[7] Zhu T, Ren H, Li A, Liu B, Cui C, Dong Y, et al. Novel bioactive glass based injectable bone cement with improved osteoinductivity and its in vivo evaluation. Sci Rep 2017;7.
[8] Sohrabi M, Eftekhari Yekta B, Rezaie H, Naimi-Jamal MR, Kumar A, Cochis A, et al. Enhancing mechanical properties and biological performances of injectable bioactive glass by gelatin and chitosan for bone small defect repair. Biomedicines 2020;8(12).
[9] Ding Y, Tang S, Yu B, Yan Y, Li H, Wei J, et al. In vitro degradability, bioactivity and primary cell responses to bone cements containing mesoporous magnesium-calcium silicate and calcium sulfate for bone regeneration. J R Soc Interface 2015;12(111).
[10] Li A, Qiu D. Phytic acid derived bioactive CaO-P2O5-SiO2 gel-glasses. J Mater Sci Mater Med 2011;22(12):2685–91.
[11] Zhao H, Liang G, Liang W, Li Q, Huang B, Li A, et al. In vitro and in vivo evaluation of the pH-neutral bioactive glass as high performance bone grafts. Mater Sci Eng C-Mat Biol Appl 2020:116.
[12] Liu W, Wu C, Liu W, Zhai W, Chang J. The effect of plaster (CaSO4 ·1/2H2O) on the compressive strength, self-setting property, and in vitro bioactivity of silicate-based bone cement. J Biomed Mater Res B Appl Biomater 2013;101(2):279–86.
[13] Wu R, Li Y, Shen M, Yang X, Zhang L, Ke X, et al. Bone tissue regeneration: the role of finely tuned pore architecture of bioactive scaffolds before clinical translation. Bioact Mater 2021;6(5):1242–54.
[14] Zhang J, Deng F, Liu X, Ge Y, Zeng Y, Zhai Z, et al. Favorable osteogenic activity of iron doped in silicocarnotite bioceramic: in vitro and in vivo Studies. J Orthop Translat 2022;32:103–11.
[15] Zhai W, Lu H, Chen L, Lin X, Huang Y, Dai K, et al. Silicate bioceramics induce angiogenesis during bone regeneration. Acta Biomater 2012;8(1):341–9.
[16] Wang M, Yang Y, Yuan K, Yang S, Tang T. Dual-functional hybrid quaternized chitosan/Mg/alginate dressing with antibacterial and angiogenic potential for diabetic wound healing. J Orthop Translat 2021;30:6–15.
[17] Xiong K, Wu T, Fan Q, Chen L, Yan M. Novel reduced graphene oxide/zinc silicate/calcium silicate electroconductive biocomposite for stimulating osteoporotic bone regeneration. ACS Appl Mater Interfaces 2017;9(51):44356–68.
[18] Cui L, Zhang J, Zou J, Yang X, Guo H, Tian H, et al. Electroactive composite scaffold with locally expressed osteoinductive factor for synergistic bone repair upon electrical stimulation. Biomaterials 2020;230:119617.
[19] Wang C, Lin K, Chang J, Sun J. Osteogenesis and angiogenesis induced by porous beta-CaSiO3/PDLGA composite scaffold via activation of AMPK/ERK1/2 and PI3K/Akt pathways. Biomaterials 2013;34(1):64–77.
[20] Zhang Y, Wang C, Fu L, Ye S, Wang M, Zhou Y. Fabrication and application of novel porous scaffold in situ-loaded graphene oxide and osteogenic peptide by cryogenic 3D printing for repairing critical-sized bone defect. Molecules 2019;24(9).
[21] Fu Z, Cui J, Zhao B, Shen SG, Lin K. An overview of polyester/hydroxyapatite composites for bone tissue repairing. J Orthop Translat 2021;28:118–30.
[22] Zakrzewski W, Dobrzynski M, Rybak Z, Szymonowicz M, Wiglusz RJ. Selected nanomaterials' application enhanced with the use of stem cells in acceleration of alveolar bone regeneration during augmentation process. Nanomaterials 2020;10(6).
[23] Jiang Y, Qin H, Wan H, Yang J, Yu Q, Jiang M, et al. Asprin-loaded strontium-containing α-calcium sulphate hemihydrate/nano-hydroxyapatite composite promotes regeneration of critical bone defects. J Cell Mol Med 2020;24(23):13690–702.
[24] Wu T, Cheng N, Xu C, Sun W, Yu C, Shi B. The effect of mesoporous bioglass on osteogenesis and adipogenesis of osteoporotic BMSCs. J Biomed Mater Res 2016;104(12):3004–14.
[25] Hou J, Fan D, Zhao L, Yu B, Su J, Wei J, et al. Degradability, cytocompatibility, and osteogenesis of porous scaffolds of nanobredigite and PCL-PEG-PCL composite. Int J Nanomed 2016;11:3545–55.
[26] Cui L, Xiang S, Chen D, Fu R, Zhang X, Chen J, et al. A novel tissue-engineered bone graft composed of silicon-substituted calcium phosphate, autogenous fine particulate bone powder and BMSCs promotes posterolateral spinal fusion in rabbits. J Orthop Translat 2021;26:151–61.
[27] Zhao D, Zhu T, Li J, Cui L, Zhang Z, Zhuang X, et al. Poly(lactic-co-glycolic acid)-based composite bone-substitute materials. Bioact Mater 2021;6(2):346–60.
[28] Lu T, Zhang J, Yuan X, Tang C, Wang X, Zhang Y, et al. Enhanced osteogenesis and angiogenesis of calcium phosphate cement incorporated with zinc silicate by synergy effect of zinc and silicon ions. Mater Sci Eng C Mater Biol Appl 2021;131:112490.
[29] Zhang F, Zhou M, Gu W, Shen Z, Ma X, Lu F, et al. Zinc-/copper-substituted dicalcium silicate cement: advanced biomaterials with enhanced osteogenesis and long-term antibacterial properties. J Mater Chem B 2020;8(5):1060–70.
[30] Omori M, Tsuchiya S, Hara K, Kuroda K, Hibi H, Okido M, et al. A new application of cell-free bone regeneration: immobilizing stem cells from human exfoliated deciduous teeth-conditioned medium onto titanium implants using atmospheric pressure plasma treatment. Stem Cell Res Ther 2015;6(1):124.
[31] Aquino-Martinez R, Artigas N, Gamez B, Luis Rosa J, Ventura F. Extracellular calcium promotes bone formation from bone marrow mesenchymal stem cells by amplifying the effects of BMP-2 on SMAD signalling. PLoS One 2017;12(5).
[32] Li L, Li J, Zou Q, Zuo Y, Cai B, Li Y. Enhanced bone tissue regeneration of a biomimetic cellular scaffold with co-cultured MSCs-derived osteogenic and angiogenic cells. Cell Prolif 2019;52(5):e12658.
[33] Xiao X, Wang W, Liu D, Zhang H, Gao P, Geng L, et al. The promotion of angiogenesis induced by three-dimensional porous beta-tricalcium phosphate scaffold with different interconnection sizes via activation of PI3K/Akt pathways. Sci Rep 2015;5:9409.
[34] Li D, Cheng P, Jiang H, Cao T, Wang J, Gao Y, et al. Vascularization converts the lineage fate of bone mesenchymal stem cells to endothelial cells in tissue-engineered bone grafts by modulating FGF2-RhoA/ROCK signaling. Cell Death Dis 2018;9(10):959.
[35] Zhu T, Jiang M, Zhang M, Cui L, Yang X, Wang X, et al. Biofunctionalized composite scaffold to potentiate osteoconduction, angiogenesis, and favorable metabolic microenvironment for osteonecrosis therapy. Bioact Mater 2022;9:446–60.
[36] Zhu T, Cui Y, Zhang M, Zhao D, Liu G, Ding J. Engineered three-dimensional scaffolds for enhanced bone regeneration in osteonecrosis. Bioact Mater 2020;5(3):584–601.
[37] Zhang Y, Xia L, Zhai D, Shi M, Luo Y, Feng C, et al. Mesoporous bioactive glass nanolayer-functionalized 3D-printed scaffolds for accelerating osteogenesis and angiogenesis. Nanoscale 2015;7(45):19207–21.
[38] Shi M, Zhou Y, Shao J, Chen Z, Song B, Chang J, et al. Stimulation of osteogenesis and angiogenesis of hBMSCs by delivering Si ions and functional drug from mesoporous silica nanospheres. Acta Biomater 2015;21:178–89.
[39] Bai L, Wu R, Wang Y, Wang X, Zhang X, Huang X, et al. Osteogenic and angiogenic activities of silicon-incorporated TiO2 nanotube arrays. J Mater Chem B 2016;4(33):5548–59.
[40] Dashnyam K, Jin G-Z, Kim J-H, Perez R, Jang J-H, Kim H-W. Promoting angiogenesis with mesoporous microcarriers through a synergistic action of delivered silicon ion and VEGF. Biomaterials 2017;116:145–57.